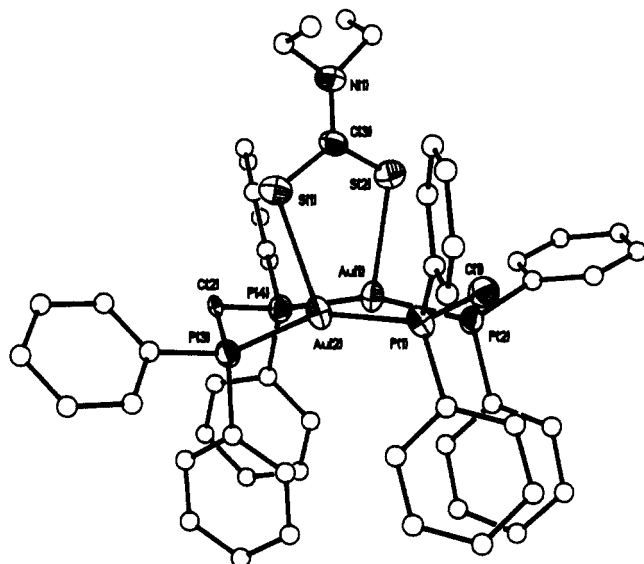


**Figure 2.** Structure of the cation of  $[\text{Au}_2(\text{dppm})_2(\text{I})][\text{Au}(\text{CN})_2]$  (**3**). Only the ipso carbons are shown for the phenyl rings.



**Figure 3.** Structure of the cation of  $[\text{Au}_2(\text{dppm})_2(\text{S}_2\text{CNET}_2)][\text{BH}_3\text{CN}]$  (**4**), showing the bridging dithiocarbamate ligand.

and 3.342 (3) Å and  $\text{Au}-\text{Au}-\text{I} = 73^\circ$ . This difference must be due to different packing forces in the two compounds. Although the  $\text{Au}-\text{I}$  separation of 3.16 Å is long compared to 2.529 Å in  $\text{AuI}_2^-$ ,<sup>17</sup> the  $\text{P}-\text{Au}-\text{P}$  angles (170 and  $171^\circ$ ) are perturbed somewhat from linearity. The yellow color of **2** in solution in-

dicates that the iodide does not completely dissociate. Also, the addition of iodide changes the  $^1\text{H}$  NMR chemical shift of the methylene group from  $\delta$  4.50 to  $\delta$  4.60, and  $^2J_{\text{HCP}}$  changes from 6.4 to 4.4 Hz.

The reaction between **1** and 1 equiv of  $\text{NaS}_2\text{CNET}_2$  gave, after precipitation of  $\text{NaBH}_3\text{CN}$ , a yellow solution from which a yellow powder of  $[\text{Au}_2(\text{dppm})_2(\text{S}_2\text{CNET}_2)][\text{BH}_3\text{CN}]$  (**4**) was obtained in a 95% yield. IR spectroscopy shows the presence of  $\text{BH}_3\text{CN}^-$  as an unassociated counterion. The crystal structure (Figure 3) shows that  $\text{S}_2\text{CNET}_2^-$  bridges the two gold atoms by forming two  $\text{Au}-\text{S}$  bonds. The  $\text{Au}-\text{S}$  bond lengths, 2.648 (3) and 2.703 (3) Å, are longer than those in  $\text{Ph}_3\text{PAu}^+(\text{S}_2\text{CNET}_2)$ , 2.34 Å,<sup>11</sup> and  $(\text{Ph}_3\text{P})_2\text{Au}^+(\text{SCN})$ , 2.47 Å.<sup>18</sup> However, the  $\text{Au}-\text{S}$  interaction is stronger than the  $\text{Au}-\text{I}$  interaction, as judged by the greater deviation from linearity of the  $\text{P}-\text{Au}-\text{P}$  angles, which are 160 and  $154^\circ$  in this  $\text{Au}-\text{S}$  compound. The average  $\text{Au}-\text{P}$  distance, 2.324 Å, is nearly the same as that found in **3**, 2.319 Å. The  $\text{Au}\cdots\text{Au}$  separation in  $\text{Au}_2(\text{S}_2\text{CNET}_2)_2$  is a short 2.782 Å,<sup>11</sup> but in **4**, with just one  $\text{S}_2\text{CNET}_2^-$  ligand, it is 2.949 (1) Å, which is typical for  $[\text{Au}_2(\text{dppm})_2]^{2+}$  compounds.

The  $[\text{Au}_2(\text{dppm})_2(\text{S}_2\text{CNET}_2)]^+$  cation remains at least partially intact in solution as shown by the yellow color ( $\lambda = 420$  nm) of **4** in solution and by the changes in the NMR spectra. The  $^1\text{H}$  NMR signal of the dppm methylene,  $\delta$  4.15, has shifted from  $\delta$  4.50 in **1**, and the  $^{31}\text{P}$  NMR signal,  $\delta$  30.0, has shifted from  $\delta$  35.9. These NMR signals are broad at room temperature, which could be due to a conformational change; the  $\text{Au}_2(\text{dppm})_2$  unit is in a boat conformation in crystals of **3** and **4** and in a chain conformation in crystals of **1**. However, ligand dissociation and reassociation could also cause the broadening.

**Acknowledgment.** We thank Drs. Raphael Raptis and Larry Falvello for assistance with the crystallography. This work was supported financially by the National Science Foundation (Grant CHE-8708625), the donors of the Petroleum Research Foundation, administered by the American Chemical Society, and the Welch Foundation.

**Registry No.** **1**, 120205-41-6; **1-2CH}\_2\text{Cl}\_2**, 120229-26-7; **2**, 120205-43-8; **3**, 120205-44-9; **4**, 120205-46-1;  $[\text{AuPPH}_3]\text{NO}_3$ , 14897-32-6;  $[\text{Au}_2(\text{dppm})_2][\text{BF}_4]_2$ , 120205-47-2.

**Supplementary Material Available:** For **1**, **3**, and **4**, tables of crystallographic data, anisotropic parameters, and hydrogen coordinates and thermal parameters (12 pages); tables of  $F_o$ ,  $F_c$ , and  $\sigma(F)$  (77 pages). Ordering information is given on any current masthead page.

(17) Braunstein, P.; Müller, A.; Bögge, H. *Inorg. Chem.* **1986**, *25*, 2104-2106.

(18) Muir, J. A.; Muir, M. M.; Arias, S. *Acta Crystallogr.* **1982**, *B38*, 1318.

Contribution from the Department of Chemistry, University Center at Binghamton, State University of New York, Binghamton, New York 13901

## Photophysical Properties of $\text{M}(\text{CO})_4(\alpha, \alpha')$ -diimine) ( $\text{M} = \text{Mo}, \text{W}$ ) Complexes

Kathleen A. Rawlins and Alistair J. Lees\*

Received October 14, 1988

Electronic absorption, emission, and excitation spectra and emission lifetimes have been recorded from a series of  $\text{M}(\text{CO})_4(\alpha, \alpha')$ -diimine) complexes [ $\text{M} = \text{Mo}, \text{W}$ ;  $\alpha, \alpha'$ -diimine = a substituted 1,10-phenanthroline (phen) ligand] in EPA glasses at 80 K and benzene at 293 K. Corresponding data have also been obtained from  $\text{M}(\text{CO})_4(\text{en})$  complexes ( $\text{M} = \text{Mo}, \text{W}$ ; en = ethylenediamine). The  $\text{M}(\text{CO})_4(\text{phen})$  complexes exhibit a broad low-energy absorption band that comprises three metal to ligand charge-transfer (MLCT) transitions ( $b_2 \rightarrow b_2^*$ ,  $a_1 \rightarrow b_2^*$ ,  $a_2 \rightarrow b_2^*$ ). A band is also observed at higher energy containing both MLCT ( $a_2 \rightarrow a_2^*$ ) and ligand field (LF) transitions. Obtained emission and excitation data at 80 K identify radiative transitions from each of the  $^3\text{MLCT}$  and  $^3\text{LF}$  components. In solution at 293 K all of the  $^3\text{MLCT}$  levels are in thermal equilibrium; however, the  $^3\text{LF}$  level remains nonequibrated. In comparison,  $\text{W}(\text{CO})_4(\text{en})$  emits only at 80 K, apparently from a single  $^3\text{LF}$  level. Further details of the emission assignments and excited-state dynamics of the  $\text{M}(\text{CO})_4(\alpha, \alpha')$ -diimine) system are discussed within.

### Introduction

Photophysical characteristics of transition-metal complexes are in many ways very different from those of organic molecules. For

example, in metal complexes a wide variety of excited states may occur, including transitions that are metal-centered, intraligand, or charge-transfer between the metal and ligands. Furthermore,

intersystem crossing is usually extremely efficient for metal complexes and it is normally expected that their lowest energy excited states are rapidly populated. Often these levels are closely spaced in energy, and the nature of the lowest lying state is not readily identified. Thus, measurements of the emission parameters can be invaluable in determining the lowest lying excited-state levels and their dynamic processes.

Numerous reports have appeared concerning excited-state behavior of transition-metal organometallic complexes that possess lowest lying metal to ligand charge-transfer (MLCT) excited states.<sup>1</sup> Many of these complexes exhibit luminescence in low-temperature frozen glasses, and a number of complexes are now recognized to emit in room-temperature solution. The M(CO)<sub>4</sub>(α,α'-diimine) (M = Cr, Mo, W) system is particularly interesting because it gives rise to unusual dual emission features in fluid solution.<sup>2</sup> Although this is the first metal carbonyl system recognized to be multiply emissive at room temperature, the detailed photophysical properties of these molecules are complicated and have not yet been fully resolved.

The present work examines closely the photophysical behavior of several M(CO)<sub>4</sub>(α,α'-diimine) complexes, where M = Mo or W and α,α'-diimine is ethylenediamine (en), 4-methyl-1,10-phenanthroline (4-Me-phen), 5-methyl-1,10-phenanthroline (5-Me-phen), or 4,7-diphenyl-1,10-phenanthroline (4,7-Ph<sub>2</sub>-phen). Absorption, emission, and excitation data have been obtained over a range of temperatures and solution environments. Through this study we are able to gain an insight into the photophysical characteristics and excited-state dynamics of the M(CO)<sub>4</sub>(α,α'-diimine) system.

### Experimental Section

**Materials.** The metal hexacarbonyls were obtained from Strem Chemical Co. and purified by sublimation. The substituted phen ligands were obtained from Alfa Chemical Co. at >99% purity and were used without further purification. The en ligand was obtained from Aldrich Chemical Co. and distilled immediately prior to use. Benzene used was high-purity Phorex grade (Baker Chemical Co.) and EPA (5:5:2 ether-isopentane-ethanol) was made from rigorously dried solvent components that had been repeatedly distilled to remove emitting impurities. Neutral alumina (80–200 mesh) used in chromatographic purifications was obtained from Fisher Scientific Co. Nitrogen used for purging was dried and deoxygenated according to a previously described method.<sup>3</sup>

**Syntheses.** The M(CO)<sub>4</sub>(α,α'-diimine) complexes, where L = substituted phen, were photochemically prepared as described previously.<sup>2,4</sup> The M(CO)<sub>4</sub>(en) complexes were synthesized according to a previously reported thermal procedure.<sup>5</sup> All compounds were carefully purified by column chromatography on neutral alumina. Infrared spectra recorded from the complexes are in accordance with the literature.<sup>2a,4,5</sup>

**Spectroscopic Measurements.** Infrared spectra were recorded on a Perkin-Elmer Model 283B spectrometer. Electronic absorption spectra were obtained on either a Perkin-Elmer Model 559 or Hewlett-Packard Model 8450A UV-visible spectrometer; reported maxima are accurate to ±2 nm. Emission and excitation spectra were recorded on a SLM Instruments Model 8000/8000S dual-monochromator spectrometer, which incorporates photon-counting facilities. The photomultiplier tube used in these experiments was a Hamamatsu R928. Emission and excitation spectra were corrected for wavelength variations in detector response and exciting-lamp intensity, respectively. Reported emission band maxima were reproducible to ±4 nm for the high-energy bands and ±8 nm for the low-energy bands. Excitation maxima were found to be reproducible to ±4 nm. Prior to the taking of emission measurements, the samples were each filtered through a 0.22-μm Millipore filter and deoxygenated by N<sub>2</sub>-purging for 15 min.

Low-temperature measurements were performed by using an Oxford Instruments Model DN1704K variable-temperature liquid-nitrogen

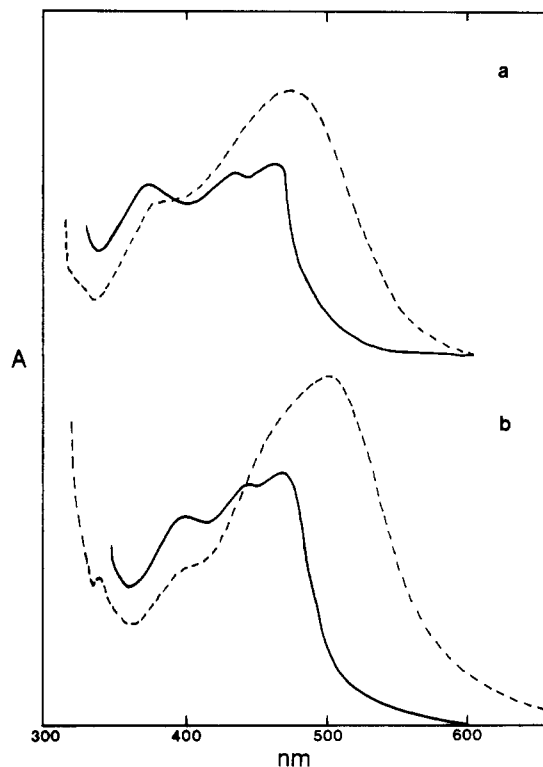


**Figure 1.** Electronic absorption spectra of (a) Mo(CO)<sub>4</sub>(5-Me-phen) and (b) W(CO)<sub>4</sub>(4-Me-phen) in (—) EPA glasses at 80 K and (---) benzene at 293 K.

**Table I.** Electronic Absorption Maxima for M(CO)<sub>4</sub>(α,α'-diimine) Complexes in EPA Glasses at 80 K and Benzene at 293 K<sup>a</sup>

complex	λ <sub>max</sub> , nm	
	benzene, 293 K	EPA, 80 K
Mo(CO) <sub>4</sub> (4-Me-phen)	338, 395 (sh), 482	392, 436
Mo(CO) <sub>4</sub> (5-Me-phen)	344, 398 (sh), 490	387, 448, 472
Mo(CO) <sub>4</sub> (4,7-Ph <sub>2</sub> -phen)	352, 420, 504	346, 388, 434, 480
Mo(CO) <sub>4</sub> (en)	305, 400	308, 397
W(CO) <sub>4</sub> (4-Me-phen)	340, 390 (sh), 500	398, 444, 468
W(CO) <sub>4</sub> (4,7-Ph <sub>2</sub> -phen)	352, 402, 519	348, 390, 440, 458, 500
W(CO) <sub>4</sub> (en)	400, 460 (sh)	400, 450

<sup>a</sup>sh = shoulder.

cryostat fitted with synthetic sapphire inner windows and quartz outer windows. Each sample was deaerated by a successive freeze-pump-thaw procedure; the sample solution was contained in a fused-quartz 1-cm cell and maintained to ±0.2 K by means of an Oxford Instruments Model 3120 controller.

Emission lifetimes were measured on a PRA System 3000 time-correlated pulsed single-photon-counting apparatus.<sup>6</sup> Sample solutions were excited with 400-nm light from a PRA Model 510 nitrogen flash lamp transmitted through an Instruments SA Inc. H-10 monochromator. Emitted light was detected at 90° via a second H-10 monochromator transmitted onto a thermoelectrically cooled red-sensitive Hamamatsu R955 photomultiplier tube, and the resulting photon counts were stored on a Tracor Northern Model 7200 microprocessor-based multichannel analyzer. The instrument response function was subsequently deconvoluted from the emission data to yield an undisturbed decay that was fitted by means of a least-squares procedure on an IBM-PC. Several of the emission decays were observed to be double-exponential, and these were resolved into their emission lifetime components by using PRA deconvolution software. Reported lifetimes were, in each instance, reproducible to ±10% over at least three measurements.

### Results

Figure 1 depicts electronic absorption spectra recorded from Mo(CO)<sub>4</sub>(5-Me-phen) and W(CO)<sub>4</sub>(4-Me-phen) in EPA glasses

- (1) (a) Geoffroy, G. L.; Wrighton, M. S. *Organometallic Photochemistry*; Academic: New York, 1979. (b) Lees, A. J. *Chem. Rev.* **1987**, *87*, 711.
- (2) (a) Manuta, D. M.; Lees, A. J. *Inorg. Chem.* **1983**, *22*, 572; **1986**, *25*, 1354. (b) Servaas, P. C.; van Dijk, H. K.; Snoeck, T. L.; Stufkens, D. J.; Oskam, A. *Inorg. Chem.* **1985**, *24*, 4494.
- (3) Schadt, M. J.; Lees, A. J. *Inorg. Chem.* **1985**, *24*, 2942.
- (4) (a) Bock, H.; tom Dieck, H. *Angew. Chem.* **1966**, *78*, 549. (b) Bock, H.; tom Dieck, H. *Chem. Ber.* **1967**, *100*, 228. (c) Brunner, H.; Hermann, W. A. *Chem. Ber.* **1972**, *105*, 770. (d) Wrighton, M. S.; Morse, D. L. *J. Organomet. Chem.* **1975**, *97*, 405.
- (5) Kraihanzel, C. S.; Cotton, F. A. *Inorg. Chem.* **1963**, *2*, 533.

- (6) O'Connor, D. V.; Phillips, D. *Time-Correlated Single Photon Counting*; Academic: London, 1984.

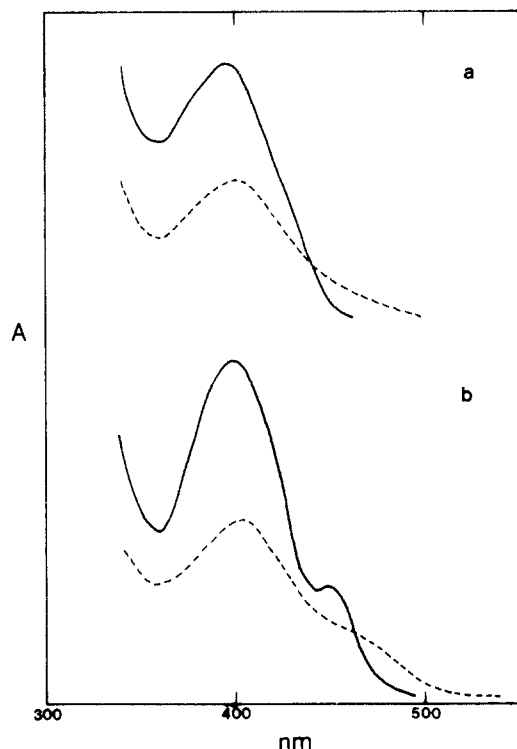


**Figure 2.** Electronic absorption spectra of (a)  $\text{Mo}(\text{CO})_4(\text{en})$  and (b)  $\text{W}(\text{CO})_4(\text{en})$  in (—) EPA glasses at 80 K and (---) benzene at 293 K.

**Table II.** Emission Maxima for  $\text{M}(\text{CO})_4(\alpha, \alpha'$ -diimine) Complexes in EPA Glasses at 80 K and Deoxygenated Benzene at 293 K<sup>a</sup>

complex	$\lambda_{\text{max}}$ , nm		
	benzene, 293 K	EPA, 293 K	EPA, 80 K
$\text{Mo}(\text{CO})_4(4\text{-Me-phen})$	546, 752	553, 765	533, 647
$\text{Mo}(\text{CO})_4(5\text{-Me-phen})$	568, 764	572, 772	530, 658
$\text{Mo}(\text{CO})_4(4,7\text{-Ph}_2\text{-phen})$	582, 770	585, 785	545 (sh), 660
$\text{Mo}(\text{CO})_4(\text{en})$	<i>b</i>	<i>b</i>	<i>b</i>
$\text{W}(\text{CO})_4(4\text{-Me-phen})$	585, 782	584, >780	527, 677
$\text{W}(\text{CO})_4(4,7\text{-Ph}_2\text{-phen})$	595, 780	595, >800	550 (sh), 675
$\text{W}(\text{CO})_4(\text{en})$	<i>b</i>	<i>b</i>	542

<sup>a</sup>Excitation wavelength is 400 nm, and the spectra are fully corrected for wavelength variations in detector response; sh = shoulder.  
<sup>b</sup>No emission observed.

at 80 K and benzene at 293 K; these spectra are typical of those observed from the series studied. On cooling, the lowest energy absorption blue shifts and reveals distinct band structure. Electronic absorption spectra of  $\text{M}(\text{CO})_4(\text{en})$  ( $\text{M} = \text{Mo}, \text{W}$ ) have also been recorded for comparison, and these are depicted in Figure 2. The absorption spectra of the substituted phen complexes are dominated by intense low-energy absorptions ( $\epsilon_{\text{max}} \sim 7000\text{--}11\,000 \text{ M}^{-1} \text{ cm}^{-1}$ ) whereas the visible transitions of the en complexes are much weaker ( $\epsilon_{\text{max}} \sim 1400\text{--}1700 \text{ M}^{-1} \text{ cm}^{-1}$ ).<sup>2,4d</sup> Absorption spectra obtained from all the complexes at 80 and 293 K are summarized in Table I.

Emission spectra recorded on 400-nm excitation of  $\text{W}(\text{CO})_4(4\text{-Me-phen})$  in an EPA glass at 80 K and deoxygenated benzene at 293 K are shown in Figure 3. These spectra are representative of the substituted phen series; in each case two emission bands are observable, a weak higher energy (HE) feature and a substantially more intense lower energy (LE) band. On cooling of an EPA solution from 293 to 150 K, the intensity ratio of these bands remains virtually unaltered; however, when the solution passes through the glass transition temperature (120–140 K) to 80 K, the emission intensity increases approximately 100-fold, the LE band becomes even more dominant, and both bands blue shift significantly. In comparison, the  $\text{W}(\text{CO})_4(\text{en})$  complex was observed to emit only in an EPA glass at 80 K, apparently from a single level. The  $\text{Mo}(\text{CO})_4(\text{en})$  complex was not observed to be

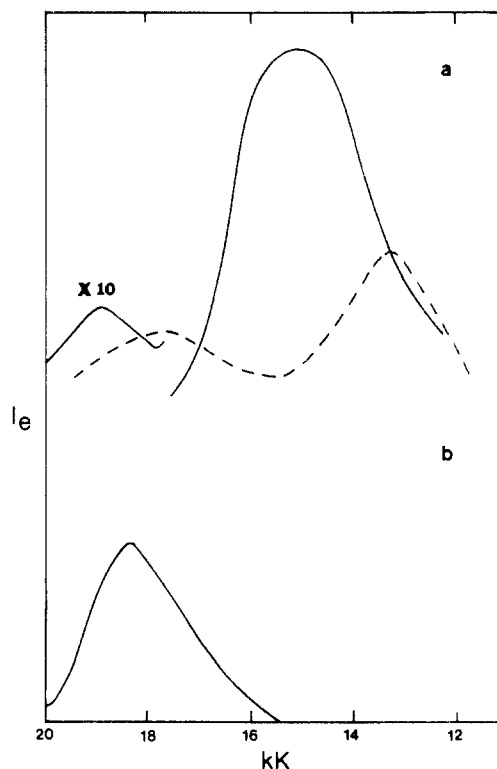


**Figure 3.** Emission spectra of (a)  $\text{W}(\text{CO})_4(4\text{-Me-phen})$  and (b)  $\text{W}(\text{CO})_4(\text{en})$  in (—) EPA glasses at 80 K and (---) deoxygenated benzene at 293 K. The excitation wavelength is 400 nm. Emission spectra at 80 K are fully corrected for wavelength variations in detector response; emission spectrum at 293 K is uncorrected. The emission intensity of  $\text{W}(\text{CO})_4(4\text{-Me-phen})$  at low temperature is approximately 100 times more intense than that at room temperature. No emission is observed from  $\text{W}(\text{CO})_4(\text{en})$  at room temperature.

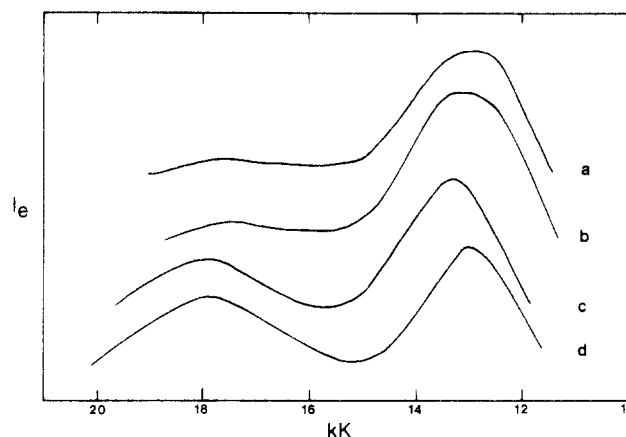


**Figure 4.** Emission spectra of  $\text{W}(\text{CO})_4(4\text{-Me-phen})$  in deoxygenated benzene at 293 K. Excitation wavelengths are (a) 475, (b) 450, (c) 400, and (d) 350 nm. Emission spectra are uncorrected for detector response; the LE band is slightly blue-shifted on 400-nm excitation due to interference from solvent scatter.

emissive, even in an EPA glass at 80 K. Emission maxima determined from all of the complexes at both low and room temperature following 400-nm excitation are listed in Table II.

Excitation wavelength variations were investigated for all of the complexes; spectra recorded from  $\text{W}(\text{CO})_4(4\text{-Me-phen})$  are illustrated in Figure 4. Data obtained from  $\text{Mo}(\text{CO})_4(5\text{-Me-phen})$  and  $\text{W}(\text{CO})_4(4\text{-Me-phen})$  at 80 and 293 K are representative of the series studied and are shown in Table III. When the exciting wavelength is varied between 350 and 475 nm, both the Mo and W complexes exhibit substantial changes in the intensities of their HE and LE bands at 293 K, with the HE band becoming relatively more intense on using shorter excitation wavelengths (see Figure 4 and Table III). In EPA glasses at 80

**Table III.** Excitation Wavelength Dependence of the Higher Energy (HE) and Lower Energy (LE) Emission Maxima of M(CO)<sub>4</sub>(α,α'-diimine) Complexes in EPA Glasses at 80 K and Deoxygenated Benzene at 293 K

complex	λ <sub>ex</sub> , nm	λ <sub>max</sub> , <sup>a</sup> nm			
		EPA, 80 K <sup>b</sup>		benzene, 293 K <sup>c</sup>	
		HE	LE	HE	LE
Mo(CO) <sub>4</sub> (5-Me-phen)	350	526 (1)	662 (8)	556 (1)	746 (4)
	400	530 (1)	658 (40)	558 (1)	748 (7)
	450	528 (1)	656 (58)	562 (1)	742 (9)
	475	532 (1)	664 (82)	562 (1)	738 (20)
W(CO) <sub>4</sub> (4-Me-phen)	350	518 (1)	668 (8)	557 (1)	769 (2)
	400	527 (1)	677 (40)	561 (1)	753 (3) <sup>d</sup>
	450	530 (1)	672 (68)	574 (1)	766 (8)
	475	532 (1)	674 (140)	582 (1)	770 (10)

<sup>a</sup> Values in parentheses illustrate relative intensities of the HE and LE bands, with normalized HE intensity = 1. <sup>b</sup> Emission maxima from spectra fully corrected for wavelength variations in detector response. <sup>c</sup> Emission maxima from uncorrected spectra. <sup>d</sup> Maximum slightly blue-shifted due to interference from solvent scatter.

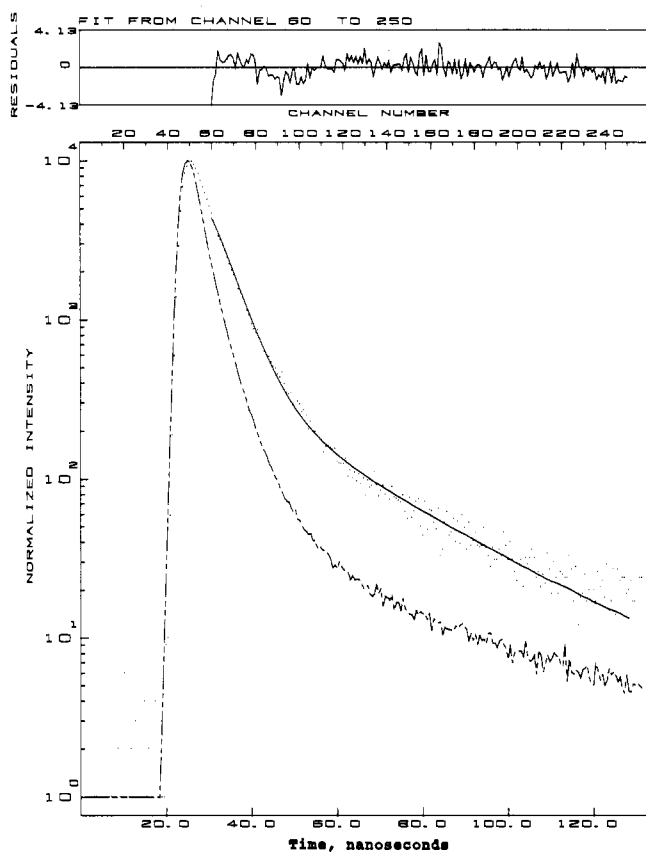


**Figure 5.** A resolved or "deconvoluted" fit of the emission decay from W(CO)<sub>4</sub>(4-Me-phen) in deoxygenated benzene at 293 K. Emission was observed at 570 nm following excitation at 390 nm. The lower curve represents the excitation lamp profile. The weighted residuals of the calculated curve with the experimental data are shown above the curves. For the data shown the residuals are randomly scattered about zero.

K this effect is also readily apparent. Furthermore, the HE bands of both the Mo and W complexes exhibit a tendency to shift in energy position with varying excitation wavelength. This effect is noticeable at either 80 or 293 K, although it is a little more pronounced for the W complexes. In contrast, the positions of the LE bands are invariant, within the experimental errors, on changing excitation wavelength at either 80 or 293 K. The emission spectrum recorded from the W(CO)<sub>4</sub>(en) complex at 80 K exhibits no dependence on excitation wavelength between 350 and 450 nm.

Emission lifetimes have been obtained from both the HE and LE emission bands of several complexes at 80 and 293 K, and the results are summarized in Table IV. In benzene solution at

**Table IV.** Emission Lifetimes for M(CO)<sub>4</sub>(α,α'-diimine) Complexes in EPA Glasses at 80 K and Deoxygenated Benzene at 293 K<sup>a</sup>

complex	τ <sub>e</sub> , ns benzene, 293 K		τ <sub>e</sub> , μs EPA, 80 K	
	HE	LE	HE	LE
Mo(CO) <sub>4</sub> (4-Me-phen)	6, 27	<i>b</i>	0.65, 6.6	1.1, 4.3
Mo(CO) <sub>4</sub> (5-Me-phen)	6, 28	23	0.36, 6.6	0.78, 4.2
Mo(CO) <sub>4</sub> (en)	<i>c</i>	<i>c</i>	<i>c</i>	<i>c</i>
W(CO) <sub>4</sub> (4-Me-phen)	3, 25	27	0.21, 7.1	0.59, 9.6
W(CO) <sub>4</sub> (en)	<i>c</i>	<i>c</i>	7.5	

<sup>a</sup> Lifetimes monitored at the uncorrected emission maxima, ±10%. <sup>b</sup> Emission is weak, and a reproducible lifetime was not obtained. <sup>c</sup> No emission observed.

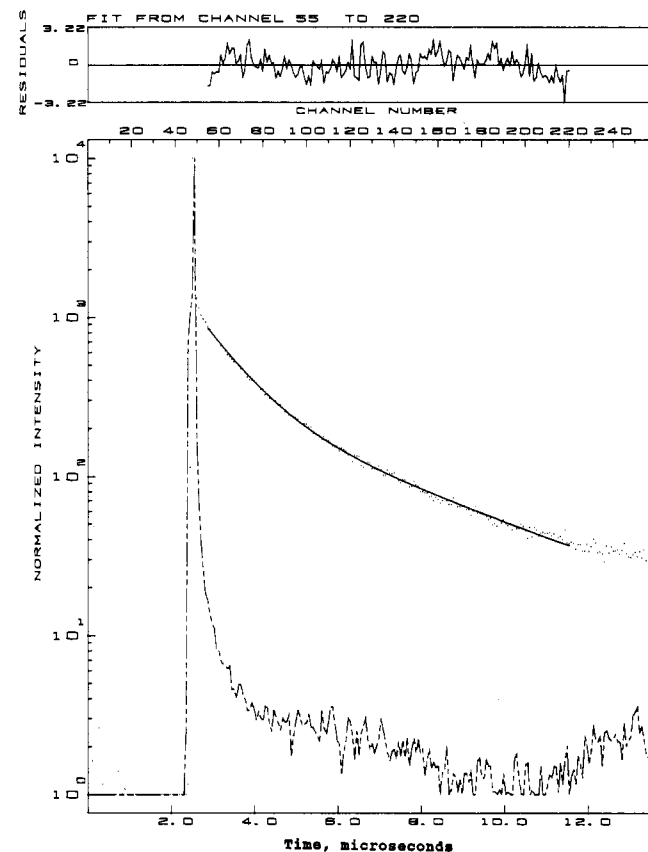


**Figure 6.** A resolved or "deconvoluted" fit of the emission decay from Mo(CO)<sub>4</sub>(4-Me-phen) in deoxygenated benzene at 293 K. Emission was observed at 750 nm following excitation at 390 nm. The lower curve represents the excitation lamp profile. The weighted residuals of the calculated curve with the experimental data are shown above the curves. For the data shown the residuals are randomly scattered about zero.

293 K the M(CO)<sub>4</sub>(α,α'-diimine) complexes exhibit emission decay curves that are single exponential at any wavelength under the LE bands and multiple exponential from the HE bands. Each HE emission decay at 293 K was monitored at the uncorrected maximum and readily resolved into two emission lifetimes (the short-lived component contributing ~85% of the emission intensity); a representative plot for W(CO)<sub>4</sub>(4-Me-phen) in benzene at 293 K is shown in Figure 5. When the short-wavelength side of the HE emission band was monitored, this decay became virtually single exponential, with the rapid lifetime component contributing up to 98% of the emission intensity. For each complex at 293 K the longer emission lifetime component obtained from the HE band corresponds, within the errors of measurement, to the emission lifetime of the LE band. At 80 K the best fits of the emission decays were found by using a double exponential for the HE bands; here the longer lifetime component typically contributes ~90% of the emission intensity. Each LE emission decay curve at 80 K, however, is more complicated and may

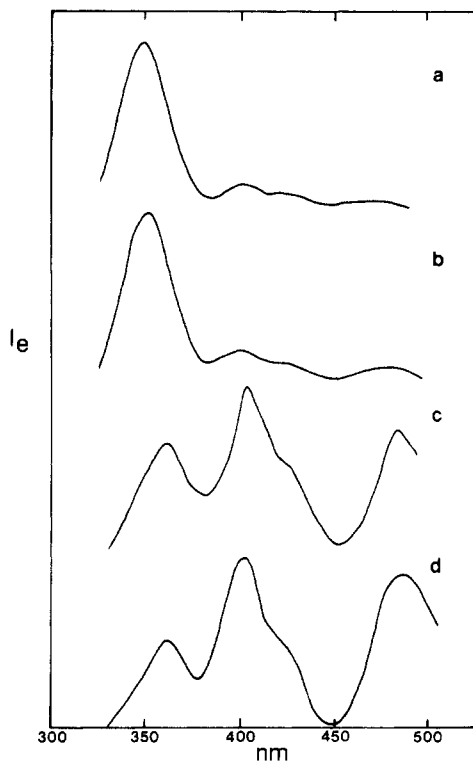


**Figure 7.** Excitation spectra of  $W(CO)_4(4\text{-Me-phen})$  in an EPA glass at 80 K. Emission is monitored at (a) 525, (b) 570, (c) 610, and (d) 650 nm. Excitation spectra are normalized following correction for wavelength variations in exciting-lamp intensity.

involve further exponentials; a typical decay curve for the LE band of  $Mo(CO)_4(4\text{-Me-phen})$  is shown in Figure 6. In each instance best fits were still obtained by using a double-exponential deconvolution, and the two lifetimes are reported in Table IV; the longer decay component typically contributes 60–70% of the emission intensity. The low-temperature emission band of  $W(CO)_4(en)$  was fitted readily to a single exponential with a lifetime of 7.5  $\mu\text{s}$  (see Table IV). This value was invariant at any wavelength under the emission band.

Excitation spectra have been recorded from the  $M(CO)_4(\alpha, \alpha'\text{-diimine})$  complexes in EPA glasses at 80 K while the wavelength of detection between the uncorrected emission maxima of the two emission bands was varied. Figure 7 illustrates excitation spectra obtained from  $W(CO)_4(4\text{-Me-phen})$ ; the other complexes in the series studied exhibit a similar trend. The spectra indicate excitation bands at approximately 350, 400, and 430 (sh) nm on monitoring at the uncorrected emission maximum (525 nm) of the HE band. Excitation bands centered at about 360, 400, 430 (sh), and 500 nm are observable on monitoring at the uncorrected emission maximum (605 nm) of the LE band, and it is noted that the latter three bands gain intensity greatly. Normalizing each of the spectra reveals that there is a smooth progression from one excitation spectrum to the other over the various detection wavelengths. For comparison, the excitation spectrum has also been recorded from the  $W(CO)_4(en)$  complex in EPA at 80 K, monitoring at its uncorrected emission maximum (530 nm); bands are observed at 350, 400, and 430 (sh) nm (see Figure 8). No change in this excitation spectral distribution was observed on varying the detection wavelength through the emission band.

## Discussion

**Excited-State Assignments.** The electronic structure of  $M(CO)_4(\alpha, \alpha'\text{-diimine})$  complexes has been studied in much detail.<sup>2,4,7</sup>

(7) (a) Saito, H.; Fujita, J.; Saito, K. *Bull. Chem. Soc. Jpn.* **1968**, *41*, 359. (b) tom Dieck, H.; Renk, J. W. *Chem. Ber.* **1971**, *104*, 110; **1972**, *105*, 1403. (c) Balk, R. W.; Stufkens, D. J.; Oskam, A. *Inorg. Chim. Acta* **1978**, *28*, 133. (d) Balk, R. W.; Stufkens, D. J.; Oskam, A. *Inorg. Chem.* **1980**, *19*, 3015.

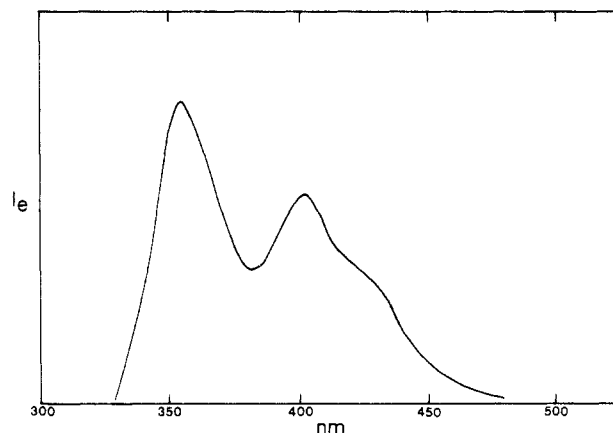


**Figure 8.** Excitation spectrum of  $W(CO)_4(en)$  in an EPA glass at 80 K. Emission is monitored at 530 nm. Excitation spectrum is fully corrected for wavelength variations in exciting-lamp intensity.

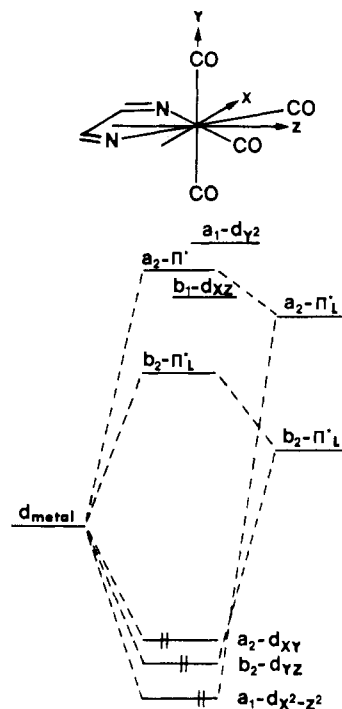


**Figure 9.** Molecular orbital scheme for  $M(CO)_4(\alpha, \alpha'\text{-diimine})$  complexes.

All of these complexes exhibit an intense metal to ligand charge-transfer (MLCT) absorption band in the visible region, and in some of these molecules the MLCT transition is extremely solvent dependent.<sup>8</sup> Through an elegant application of resonance Raman (RR) and magnetic circular dichroism (MCD) spectroscopy, Stufkens et al. have demonstrated that the low-energy MLCT band envelope actually comprises three MLCT transitions (see Figure 9), the most intense one being assigned to a  $z$ -polarized ( $d_{yz}$ )  $b_2 \rightarrow b_2(\pi^*)$  transition that is directed along the dipole vector of the complex.<sup>2b,7c</sup> The degree of solvatochromism for a range of  $M(CO)_4(\alpha, \alpha'\text{-diimine})$  complexes has been correlated with the extent of mixing of the metal  $d_{yz}$  and ligand  $\pi^*$  orbitals; increased mixing reduces the MLCT character and subsequently the solvent dependence of the  $b_2 \rightarrow b_2^*$  transition.<sup>2b</sup> For the substituted phen complexes studied here the amount of orbital mixing is thought to be relatively small and the complexes are indeed extremely solvent sensitive.<sup>2,4d,8</sup> The  $y$ -polarized ( $d_{xz}$ )  $a_1 \rightarrow b_2(\pi^*)$  and  $x$ -polarized ( $d_{xy}$ )  $a_2 \rightarrow b_2(\pi^*)$  MLCT components have also been observed in RR excitation profiles of  $M(CO)_4(\alpha, \alpha'\text{-diimine})$

(8) Manuta, D. M.; Lees, A. J. *Inorg. Chem.* **1983**, *22*, 3825; **1986**, *25*, 3212.

complexes, the latter transition being fairly weak for the substituted phen derivatives.<sup>2b</sup> For convenience, we will refer to the low-energy composite MLCT transitions as the MLCT(1) state(s).

The spectral changes observed on cooling these complexes to 80 K EPA glasses (see Figure 1 and Table I) are entirely consistent with the MLCT(1) assignment. On cooling, some band sharpening and features of some of the MLCT components can be seen. In accordance with the above interpretation the strongest two features at low temperature are assigned to the  $b_2 \rightarrow b_2^*$  and  $a_1 \rightarrow b_2^*$  MLCT transitions. For the W(CO)<sub>4</sub>(4,7-Ph<sub>2</sub>-phen) complex a third absorption feature is also observable, and this is attributed to the  $a_2 \rightarrow b_2^*$  MLCT transition. It is noted that these transitions appear to blue shift on cooling; this rigidochromism is believed to relate to the reorientation of the solvent dipoles about the metal complex as the medium becomes rigid. This environment effect or "rigidochromic" effect has been recognized for MLCT states of other carbonyl complexes.<sup>1b,9</sup>

Much less is understood about the higher energy absorptions at ~400 nm in the M(CO)<sub>4</sub>(α,α-diimine) complexes. Generally, it is thought that these transitions are predominantly of ligand field (LF) character, on the basis of the close similarity of these absorptions to those of the spectra of the M(CO)<sub>4</sub>(en) (M = Mo, W) derivatives (see Figures 1 and 2 and Table I).<sup>2,4d,7a</sup> The M(CO)<sub>4</sub>(en) complexes exhibit <sup>1</sup>LF absorptions centered at 400 nm, and the W derivative, as a result of increased spin-orbit coupling, displays a <sup>3</sup>LF shoulder (~460 nm) at 293 K, which is noticeably more pronounced (450 nm) at 80 K. However, for the substituted phen complexes it is possible that a further MLCT transition to the second  $a_2(\pi^*)$  level of the diimine ligand is also present, as predicted from the MO diagram (see Figure 9). Indeed, some evidence for the  $a_2 \rightarrow a_2^*$  transition at ~470 nm has been obtained in the MCD spectrum of W(CO)<sub>4</sub>(4,7-Ph<sub>2</sub>-phen), but this was notably absent in the RR excitation profile possibly because of interaction with the nearby <sup>3</sup>LF level.<sup>2b</sup> Hereafter, this higher energy  $a_2 \rightarrow a_2^*$  MLCT band will be referred to as the MLCT(2) state. The slight blue shift observed in the absorption band at ~400 nm on cooling to 80 K is consistent with some MLCT(2) character in a predominantly LF band. Finally, the shorter wavelength absorptions observed in the substituted phen complexes at ~330–350 nm are thought to involve LF transitions to the higher energy ( $d_{z^2}$ )<sub>1</sub> level (see Figure 9).

Emission spectra of the substituted phen complexes each exhibit two bands. Previously it has been shown that both emission bands are solvent dependent and, consequently, are believed to both contain <sup>3</sup>MLCT character.<sup>2a,10</sup> Indeed, the emission spectra observed on cooling to 80 K are consistent with MLCT assignments, as both bands blue shift significantly (see Figure 3 and Table II). MLCT emission bands are known to be especially affected when the solution changes from a dynamic to a rigid environment, an effect referred to as "luminescence rigidochromism"<sup>11</sup> and one recognized for other metal carbonyl systems.<sup>1b,9,12</sup> This phenomenon is thought to be primarily brought about by the dramatic changes in the local solvent environment through the reorientation of the solvent dipoles when the solution freezes, analogous to that noted above for the MLCT absorption bands.

The instead lower energy (LE) emission band is assigned to the MLCT(1) excited-state manifold. Excitation spectra obtained from the low-energy maxima confirm that this emission band arises from the excited states contained in the broad MLCT absorption envelope. At 293 K this band yields a single-emission lifetime (throughout the entire range of wavelengths within this band),

which indicates that the rates of interconversion between the various <sup>3</sup>MLCT components in MLCT(1) are rapid (vide infra). However, at 80 K two lifetimes are observable, attributable to the individual <sup>3</sup>MLCT levels; the most intense decay (which is the longer lifetime value at 4–10 μs) is assigned to the  $b_2 \rightarrow b_2^*$  state, and the shorter lifetime (0.59–1.1 μs) is attributed to the  $a_1 \rightarrow b_2^*$  state. Although these two appear to be the dominant emission decays at 80 K, the nature of the exponential deconvolution suggests that a third level, presumably the  $a_2 \rightarrow b_2^*$  state, is probably also contributing weakly. At either temperature no significant dependence on the excitation wavelength was observed for the energy position of the LE emission band (see Figure 4 and Table III). However, it should be recognized that this emission band is broad and red-shifted and that small energy shifts would be difficult to observe experimentally.

In contrast, the weaker higher energy (HE) emission band apparently comprises two components. At either 80 or 293 K the band position exhibits a significant dependence on the excitation wavelength (see Figure 4 and Table III) and two emission lifetimes were resolved (see Table IV). Clearly, two excited states contribute to this high-energy emission feature: the MLCT character in this band, as noted above, is assigned to the MLCT(2) state and the other component is attributed to the lowest lying <sup>3</sup>LF level. The <sup>3</sup>LF assignment is supported by the observation of an emission band at 542 nm from W(CO)<sub>4</sub>(en) at 80 K (see Figure 3) and the similarity of the excitation spectra between the substituted phen complexes and the en derivative (see Figures 7 and 8). In either the en or phen complexes the excitation bands at 400 and 430 (sh) nm are attributed to the <sup>1</sup>LF and <sup>3</sup>LF levels, respectively, and the band at ~360 nm is thought to be the upper <sup>1</sup>LF level. The <sup>1</sup>LF levels participate by nonradiatively populating the emitting <sup>3</sup>LF and <sup>3</sup>MLCT states. Although W(CO)<sub>4</sub>(en) was not found to be emissive at 293 K, and Mo(CO)<sub>4</sub>(en) did not emit at either 293 or 80 K, it is noted that the closely related W(CO)<sub>4</sub>(tmen) (tmen = *N,N,N',N'*-tetramethylethylenediamine) complex is weakly emissive at room temperature, ( $\lambda_{\max} = 543$  nm).<sup>2b</sup> Indeed, there may be increased orbital mixing in the substituted phen complexes as the <sup>3</sup>LF level would appear to be the dominant component in the HE band (vide infra).

Until lately, <sup>3</sup>LF emissions at room temperature have been largely unrecognized and thought to be extremely short-lived due to rapidly competing photodissociation mechanisms. However, recent studies of XRe(CO)<sub>4</sub>L and CpRe(CO)<sub>2</sub>L (X = Cl, I; Cp = η<sup>5</sup>-C<sub>5</sub>H<sub>5</sub>; L = P or N donor ligand) complexes have identified radiative decay from <sup>3</sup>LF states under fluid solution conditions.<sup>13</sup> Consistent with this rationale the short (3–6 ns) emission lifetime at 293 K (see Table IV) is assigned to the lowest energy <sup>3</sup>LF state. From the deconvolution of the HE emission decay this emission contributes ~85% of the overall band intensity. The other decay component at 293 K, with a lifetime of 25–28 ns, is attributed to the MLCT(2) level. The <sup>3</sup>LF state is placed above the MLCT(2) level because its rapid decay dominates the emission deconvolution on monitoring at the short-wavelength side of the HE band. At 80 K an assignment of the two emission lifetimes is more speculative. Tentatively, we attribute the weak (~10%) shorter component (0.21–0.65 μs) to the <sup>3</sup>MLCT(2) level and the intense (~90%) longer component (6.6–7.1 μs) to the <sup>3</sup>LF state. Such an assignment would be consistent with the room-temperature results and the close match with the emission lifetime and excitation spectral data of W(CO)<sub>4</sub>(en) at 80 K. Additionally, the excitation spectral progression that is observed on varying the monitoring emission wavelength suggests that these upper states effectively populate the emitting <sup>3</sup>MLCT(1) manifold at 80 K via nonradiative mechanisms. In particular, the weak emission and short lifetime of the <sup>3</sup>MLCT(2) state imply that this state very efficiently decays nonradiatively, presumably by internal conversion to the <sup>3</sup>MLCT(1) levels.

(9) (a) Zulu, M. M.; Lees, A. J. *Inorg. Chem.* **1988**, *27*, 3325. (b) Salman, O. A.; Drickamer, H. G. *J. Chem. Phys.* **1982**, *77*, 3337.

(10) Although there is ample evidence that emissions from transition-metal organometallic complexes arise from predominantly triplet-centered levels, it is noted, however, that these states cannot be described as "pure" triplets due to the heavy metal influence. See ref 1b for further discussion.

(11) (a) Wrighton, D. L.; Morse, D. L. *J. Am. Chem. Soc.* **1974**, *96*, 998. (b) Giordano, P. J.; Fredericks, S. M.; Wrighton, M. S.; Morse, D. L. *J. Am. Chem. Soc.* **1978**, *100*, 2257.

(12) Zulu, M. M.; Lees, A. J. *Inorg. Chem.* **1989**, *28*, 85.

(13) (a) Glezen, M. M.; Lees, A. J. *J. Chem. Soc., Chem. Commun.* **1987**, 1752. (b) Glezen, M. M.; Lees, A. J. *J. Am. Chem. Soc.* **1988**, *110*, 3892. (c) Glezen, M. M.; Lees, A. J. *J. Am. Chem. Soc.* **1988**, *110*, 6243.

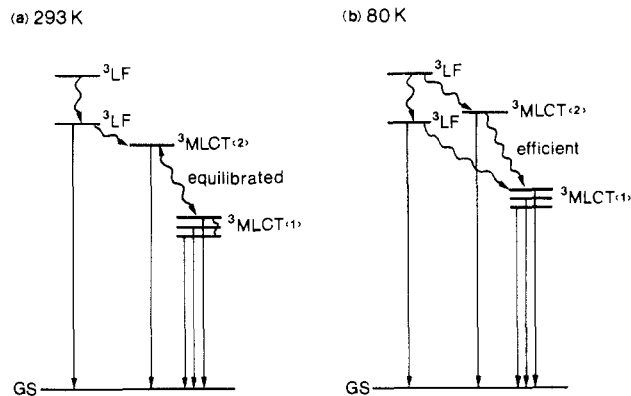


**Figure 10.** Photophysical scheme for  $M(\text{CO})_4(\alpha, \alpha'$ -diimine) complexes in (a) benzene solution at 293 K and (b) EPA glass at 80 K. Horizontal lines depict the  $^3\text{LF}$  and  $^3\text{MLCT}$  states; only the triplet levels are shown for clarity. Vertical and wavy lines denote radiative and nonradiative processes, respectively.

**Excited-State Dynamics.** The observed temperature and excitation wavelength effects on emission and excitation spectra and the recorded emission lifetimes provide an insight into the nature of the dynamic processes among the various excited-state levels.

At 293 K the lifetimes of the  $^3\text{MLCT}(1)$  and  $^3\text{MLCT}(2)$  components are equivalent, within the errors of measurement, and this indicates that these states are thermally equilibrated; i.e., the rates of interconversion between these levels are rapid compared to the rates of deactivation to the ground state.<sup>14</sup> The  $^3\text{LF}$  component in the HE band, though, has a shorter lifetime and is therefore not equilibrated with the  $^3\text{MLCT}$  levels. Indeed, the observed emission spectral behavior on varying temperature and excitation wavelength while the solution is still fluid is illustrative of a nonequilibrated system. This is because the relative intensity of the HE emission band decreases as the exciting wavelengths become longer (see Figure 4 and Table III) and the overall emission spectral distribution is virtually unchanged on lowering the temperature to 150 K, ruling out a Boltzmann thermal equilibrium. The reason for the lack of equilibrium behavior is that the  $^3\text{LF}$  emission apparently dominates the HE emission band—this conclusion is also supported by the intensity deconvolutions of the emission decays. The  $^3\text{MLCT}(2)$  band, while in thermal equilibrium with the  $^3\text{MLCT}(1)$  manifold in fluid solution, is only a minor component to the HE emission band, possibly because its Boltzmann population may be quite small. The energy difference between the 0,0 levels of these  $^3\text{MLCT}$  states is, therefore, not ascertained from our emission spectral data, but presumably it is within the recognized equilibrium limit of  $1000\text{ cm}^{-1}$ .<sup>14</sup> As previously noted for the related binuclear  $(\text{OC})_5\text{W}-\text{L}-\text{W}(\text{CO})_5$  system, the positions of the  $^3\text{MLCT}$  emission bands can be misleading with respect to the actual energies of the 0,0 levels.<sup>12</sup>

At 80 K the emission of both HE and LE bands becomes much more intense, consistent with a substantial reduction in the competing nonradiative processes. The thermal equilibrium between the  $^3\text{MLCT}(1)$  and  $^3\text{MLCT}(2)$  levels is now apparently lost as different emission lifetimes are observable, although the excitation data imply that the  $^3\text{MLCT}(2)$  state efficiently populates the  $^3\text{MLCT}(1)$  manifold by nonradiative mechanisms. Moreover, the emission lifetimes illustrate that the individual  $^3\text{MLCT}$  components in the  $^3\text{MLCT}(1)$  manifold are not thermally equilibrated in EPA glasses at 80 K.

Multiple-state emission at room temperature is becoming increasingly recognized for transition-metal complexes, and a number of systems are now known to exhibit this phenome-

non.<sup>1b,15-18</sup> Most examples, though, concern multiple emission at low temperature, and it is not uncommon to find metal complexes that are nonequilibrated in frozen solutions. The present system is unusual in that the multiple emission is observable at room temperature, and it is especially noteworthy because the participating  $^3\text{LF}$  and  $^3\text{MLCT}$  excited states are not in thermal equilibrium. This system represents the second identified case of nonequilibrated multiple emission at 293 K between  $^3\text{LF}$  and  $^3\text{MLCT}$  states, closely following our recent observations of a series of  $\text{CpRe}(\text{CO})_2\text{L}$  (L = pyridine or substituted pyridine) complexes.<sup>13c</sup> However, all of the  $^3\text{MLCT}$  states involved in the  $M(\text{CO})_4(\alpha, \alpha'$ -diimine) molecules appear to be thermally equilibrated in 293 K solution. Thus, the reason for the nonequilibration behavior may be related to orbital parentage; the vibrationally relaxed  $^3\text{LF}$  and  $^3\text{MLCT}$  states are likely to have quite different molecular geometries, and this can inhibit the rates of interconversion between these levels. A similar explanation has recently been provided for the nonequilibrated emissions of a series of mixed-ligand copper(I) complexes.<sup>16c</sup>

**Photophysical Model.** Figure 10 summarizes the experimental observations in a diagram depicting the excited states involved in the deactivation of  $M(\text{CO})_4(\alpha, \alpha'$ -diimine) complexes. In either scheme the corresponding singlet states are not illustrated for reasons of clarity; these states are expected to relax rapidly to their triplets.<sup>10</sup> In (a) the photophysical properties of the complexes in 293 K solution are illustrated. The  $^3\text{MLCT}(1)$  manifold lies significantly below the other states; the individual  $^3\text{MLCT}$  components are shown to be thermally equilibrated with each other and with the upper emitting  $^3\text{MLCT}(2)$  level. The  $^3\text{LF}$  state is shown to lie just above the  $^3\text{MLCT}(2)$  level in accordance with the measured emission decay deconvolutions. A radiative transition is depicted from the  $^3\text{LF}$  state consistent with the short lifetime observed. In (b) the photophysical properties of the complexes in frozen glasses are depicted. The  $^3\text{MLCT}(1)$  and  $^3\text{MLCT}(2)$  states are raised in energy relative to those of the  $^3\text{LF}$  levels, and the whole system is shown to be nonequilibrated, although it is recognized that the  $^3\text{MLCT}(2)$  level efficiently deactivates to the  $^3\text{MLCT}(1)$  manifold. In accordance with the excitation spectral data a higher  $^3\text{LF}$  state is included in both schemes, but its only photophysical contribution is to nonradiatively populate the lower lying  $^3\text{LF}$  and  $^3\text{MLCT}$  levels.

**Acknowledgment.** We are grateful to the donors of the Petroleum Research Fund, administered by the American Chemical Society, for support of this research.

**Registry No.**  $\text{Mo}(\text{CO})_4(4\text{-Me-phen})$ , 101056-25-1;  $\text{Mo}(\text{CO})_4(5\text{-Me-phen})$ , 35270-49-6;  $\text{Mo}(\text{CO})_4(4,7\text{-Ph}_2\text{-phen})$ , 16632-93-2;  $\text{Mo}(\text{CO})_4(\text{en})$ , 31298-40-5;  $\text{W}(\text{CO})_4(4\text{-Me-phen})$ , 87655-71-8;  $\text{W}(\text{CO})_4(4,7\text{-Ph}_2\text{-phen})$ , 83005-95-2;  $\text{W}(\text{CO})_4(\text{en})$ , 31404-74-7.

- (15) (a) For a review of literature appearing up to 1980, see: DeArmond, M. K.; Carlin, C. M. *Coord. Chem. Rev.* **1981**, *36*, 325. (b) Segers, D. P.; DeArmond, M. K.; Grutsch, P. A.; Kutal, C. *Inorg. Chem.* **1984**, *23*, 2874. (c) Blakley, R. L.; Myrick, M. L.; DeArmond, M. K. *J. Am. Chem. Soc.* **1986**, *108*, 7843.
- (16) (a) Rader, R. A.; McMillin, D. R.; Buckner, M. T.; Matthews, T. G.; Casadonte, D. J.; Lengel, R. K.; Whittaker, S. B.; Darmon, L. M.; Lytle, F. E. *J. Am. Chem. Soc.* **1981**, *103*, 5906. (b) Kirchhoff, J. R.; Gammache, R. E.; Blaskie, M. W.; Del Paggio, A. A.; Lengel, R. K.; McMillin, D. R. *Inorg. Chem.* **1983**, *22*, 2380. (c) Casadonte, D. J.; McMillin, D. R. *J. Am. Chem. Soc.* **1987**, *109*, 331.
- (17) (a) Watts, R. J. *Inorg. Chem.* **1981**, *20*, 2302. (b) Sexton, D. A.; Ford, P. C.; Magde, D. *J. Phys. Chem.* **1983**, *87*, 197. (c) Nishizawa, M.; Suzuki, T. M.; Sprouse, S.; Watts, R. J.; Ford, P. C. *Inorg. Chem.* **1984**, *23*, 1837.
- (18) (a) Kirk, A. D.; Porter, G. B. *J. Phys. Chem.* **1980**, *84*, 887. (b) Breddels, P. A.; Berdowski, P. A. M.; Blasse, G. *J. Chem. Soc., Faraday Trans. 2* **1982**, *78*, 595. (c) Martin, M.; Krogh-Jespersen, M.-B.; Hsu, M.; Tewksbury, J.; Laurent, M.; Viswanath, K.; Patterson, H. *Inorg. Chem.* **1983**, *22*, 647. (d) Belser, P.; von Zelewsky, A.; Juris, A.; Barigelletti, F.; Balzani, V. *Chem. Phys. Lett.* **1984**, *104*, 100.

(14) Kemp, T. J. *Prog. React. Kinet.* **1980**, *10*, 301.